

1 **Estimation of Poisson's ratio and variation of tensile yield strength of composite clay**
2 **balls used in pebble matrix filtration**

3 **Jay Rajapakse**, Lecturer, Science and Engineering Faculty, Queensland University of
4 Technology, 2 George Street, GPO Box 2434, Brisbane Qld 4001, Australia.

5

6 **Chaminda Gallage**, Senior Lecturer, Science and Engineering Faculty, Queensland
7 University of Technology, 2 George Street, GPO Box 2434, Brisbane Qld 4001, Australia.

8

9 **Biyavilage Dareeju**, Doctoral Candidate, Science and Engineering Faculty, Queensland
10 University of Technology, 2 George Street, GPO Box 2434, Brisbane Qld 4001, Australia.

11

12 **Gopal Madabhushi**, Professor, Engineering Department, University of Cambridge,
13 Trumpington Street, Cambridge CB2 1PZ

14

15 **Richard Fenner**, Reader, Engineering Department, University of Cambridge, Trumpington
16 Street, Cambridge CB2 1PZ

17

18

19

20

21 **Abstract:** Clay balls can be used as alternatives to natural pebbles in pebble matrix filtration,
22 a device for drinking water treatment. These clay balls are subjected to stresses due to self-
23 weight and overburden in water saturated conditions. Although there are empirical
24 relationships for evaluating tensile yields strength (Ts) of clay balls using Poisson's ratio (μ),
25 diameter (d) of clay balls, and failure polar force (Fs), so far for such calculations the value of
26 Poisson's ratio (μ) was taken from studies based on clay bricks. However, during ball
27 preparation if clay is mixed with other raw materials from industry wastes such as saw dust or
28 alum sludge in order to enhance the pollutant removal properties of the filter media, then the
29 Poisson's ratio (μ) of composite balls would be quite different to that of clay bricks. This
30 paper describes a novel method for estimating Poisson's ratio (μ) of composite clay balls by
31 measuring vertical deformation using linear variable displacement transducers (LVDTs) in
32 uniaxial compressive strength (UCS) apparatus and lateral deformation using particle image
33 velocimetry (PIV).

34

35 **Keywords:** *Composite clay balls, Poisson ratio, PIV, Tensile yield strength, Pebble Matrix*
36 *Filtration, Filter media*

37

38 **Introduction**

39 Pebble matrix filtration (PMF), a pre-filtration method for high turbidity removal of surface
40 waters has found effective both in the laboratory and in field scales (Rajapakse and Ives
41 1990; Rajapakse and Ives 2003; Rajapakse et al. 2005; Rajapakse and Fenner 2011;
42 Rajapakse et al. 2012). Selection of suitable filter material for PMF, especially for a rural
43 water treatment process is challenging due to local availability of natural pebbles and sand

44 with required particle sizes and their distributions. Hand-made clay pebbles (balls) is an
45 alternative to natural pebbles in filter media in terms of low cost and environmental
46 sustainability, especially where natural pebbles are not readily available. The use of mono-
47 medium clay balls as a new filter media has been tested in the laboratory (Rajapakse and
48 Fenner 2011) and the strength properties of mono-medium clay balls have been discussed in
49 Rajapakse et al., 2012. To further enhance the pollutant removal ability of these clay balls
50 which were made of clay, a material known as brick mix (BM), some waste materials such as
51 saw dust, red mud, water treatment alum sludge, shredded paper, and sugar mulch were
52 added to the BM at various proportions (Rajapakse et al. 2015). The strength properties of
53 these composite clay balls were evaluated using uniaxial compression test.

54 Pressure and viscous (drag) force due to flow, gravity and uplift forces however
55 impose on the filter media (Indraratna and Radampola 2002). These clay balls within a filter
56 bed are subjected to stresses due to self-weight and overburden, therefore, it is important that
57 clay balls should be able to withstand these stresses in water under saturated conditions.
58 Rajapakse et al. (2012) highlighted that the tensile yield strength (T_s) of clay pebbles should
59 provide a factor of safety against self-weight and overburden pressure of the PMF. Sternberg
60 and Rosenthal (1952) developed an expression to evaluate tensile yield strength (T_s) of clay
61 pebbles using Poisson's ratio (μ), diameter (d), and failure polar force (F_s) as given in Eq 1.
62 During the compression test, the strength of a clay ball depends on the tensile strength in a
63 cross sectional plane along the loading axis. The maximum tensile strength was defined as
64 the tensile yield strength of a clay ball. Compression force (Polar force) was an indirect
65 measurement of the tensile strength of a clay ball during testing. The maximum polar force
66 was defined as the failure polar force in this study.

67

$$T_s = \frac{0.3317 F_s}{d^2} \left(\frac{14+5\mu}{7+5\mu} \right) \quad (1)$$

68 The value of Poisson's ratio of clay pebbles however were based on the clay bricks in
69 estimating the tensile yield strength in the previous studies. Although the Poisson ratio of
70 clay bricks may be taken as approximately similar to the mono-medium clay balls, when clay
71 is mixed with other additives, the composite clay balls would not have the same properties as
72 mono-medium clay balls. In this study, UCS apparatus was used for crushing clay balls and
73 vertical deformation was measured using both linear variable displacement transducers
74 (LVDTs) and particle image velocimetry (PIV), whereas lateral deformation was measured
75 using particle image velocimetry (PIV) only. After establishing a good correlation between
76 the vertical LVDT and the PIV measurements, the results were used to calculate Poisson's
77 ratio of composite material in tensile yield strength test under the uniaxial loading conditions.

78 **Laboratory Experiments**

79 *Lateral Deformation Measurement using PIV*

80 In recent years, digital image correlation method became more applicable in non-contact
81 deformation measurements (Pan et al. 2009). Due to higher cost in contact deformation
82 measurements of the composite clay balls in lateral direction, the PIV method, which was
83 originally developed for measuring velocity of fluids (Adrian 1991) and later modified for
84 evaluation of natural soil particle movement (While and Take 2002), was used in this study.
85 This method was implemented to analyse the image sequence and it quantifies the
86 development of volumetric and shear strains within the interface shear zone (Westgate and
87 DeJong 2006). The PIV analysis procedure summarized by Hosseini et al. (2014) was
88 followed here. Application of the GeoPIV software developed by White and Take (White et
89 al. 2003) in analyzing digital images in the PIV method for strain calculation was highlighted
90 by Bandula-Heva and Dhanasekar (2011) and the use of the GeoPIV is described in detail by
91 Madabhushi (2014).

92 For the PIV analysis, the composite clay balls were tested under monotonic loading
93 conditions at a constant displacement rate (1mm/min) to ensure static loading requirements.
94 Fig. 1 illustrates the experimental setup used for measuring lateral strain of the composite
95 clay pebbles. Digital images of clay pebbles were taken every five seconds (0.20Hz), using a
96 canon EOS 450D computerized camera under consistent camera settings; appropriate
97 continuous light intensity, camera shutter speed, and zero manual intervention of camera.
98 Both time-load history, time-displacement history under the UCS test conditions and time-
99 digital image history under the PIV test conditions were obtained for each composite clay
100 balls during the loading.

101

102 Digital images taken at a constant time interval from beginning to yield point were
103 used for the PIV analysis to evaluate lateral strain of composite clay balls. Fig. 2 shows the
104 grid of patches of an input digital image developed in the PIV analysis, with a typical size of
105 a patch as 120×120 pixels. Based on the investigations of White et al. (2003), the precision
106 error, ρ_{pixel} , can be calculated using following equation:

107

$$108 \quad \rho_{pixel} = \frac{0.6}{L} + \frac{150,000}{L^8} \quad (2)$$

109 Where, L is patch size. Here, error is 0.0005 pixels, which is less than standard error
110 of 0.0007 pixels (Hosseini et al. 2014). Size of grid, patches, and distance between patches
111 depends on the requirement of analysis and quality of digital images. Both vertical and lateral
112 strains were evaluated in this study, adopting the method proposed by Bandula-heva and
113 Dhanasekar (2011) and Thamboo et al. (2013). Key critical task of this analysis however was
114 to minimize the error by 3-D effects of clay pebbles in calculating plane strain in the PIV

115 analysis. Previous PIV studies were associated only with plane strain elements such as square
116 and rectangular blocks (Bandula-heva and Dhanasekar 2011; Thamboo et al. 2013). To
117 minimize these effects, two precautions were taken as follows: 1) in calculating vertical
118 strain, two reference points were introduced to each loading plate of uniaxial compression
119 apparatus as shown in Fig. 2 and vertical strain of clay pebbles were determined using these
120 four reference points, 2) in calculating horizontal strain, reference patches along neutral axis
121 (diameter) were selected for calculation.

122

123 *Comparison of deformation measured using LVDT and PIV method*

124 Fig. 3 illustrates the comparison of vertical strain calculated using the PIV method and
125 experiments results from the USC test using the LVDT for different three clay balls.
126 Elasticity behavior of specimens in Test 2 and Test 3 shows a similar behavior as same
127 material type used in these two experiments with two different pebble sizes, where Test 3 has
128 a higher diameter than Test 2 experiencing higher time for crushing as shown in Fig. 3.
129 Materials used in Test 1 are altered from Test 2 & Test 3, resulting a diversion of elastic
130 behavior from Test 2 and Test 3. According to Fig. 3, vertical strain values calculated using
131 the PIV analysis method shows a minor deviation with experimental strain values obtained
132 from USC test results. The fluctuation of the PIV vertical strain values in Fig. 3 from
133 experimental strain values may be as a results of uncertainties associated with experimental
134 conditions such as light intensity and humidity, defects in digital camera, and uncertainties in
135 the PIV analysis. Considering this good agreement in vertical strain values shown in Fig. 3,
136 the PIV method was used in remaining analyses in this paper to evaluate the lateral strain of
137 the composite clay pebble materials in Poisson's ratio calculation.

138 As the PIV method is suitable to evaluate vertical and lateral strain of composite clay
139 pebbles, these two strain values were calculated for each composite clay pebble type. Fig. 4
140 illustrates the distribution of vertical strain and lateral strain of a typical composite clay
141 pebbles and Poisson's ratio of clay pebbles were evaluated using these distribution. Key
142 reasons for some scattered points in distribution between vertical and lateral strain values are
143 uncertainties in the PIV analysis and the test environment as explained earlier and the
144 impurities in hand-made clay pebbles, especially with those made with three industry wastes.

145

146 **Strength Characteristics Analysis**

147 *Tensile yield strength Measurement*

148 According to Sternberg and Rosenthal's (1952), tensile yield strength of a ball is a
149 function of failure polar force, Poisson's ratio and ball diameter (Eq. 1). An experimental
150 setup was proposed in this study to evaluate the validation of this expression on the clay
151 pebbles, prior to estimate the tensile yield strength of the composite clay pebbles. With same
152 constant Poisson's ratio, the tensile yield strength can be simply estimated using the slope of
153 failure polar force verses square pebble diameter distribution as given in Eq. 3, which is a
154 rearranged version of Eq. 1.

$$155 \quad F_s = \left(\frac{7+5\mu}{.0331*(14+5\mu)} \right) d^2 T_s \quad (3)$$

156 Fig. 5 illustrates the variation of failure polar force with square diameter of five clay
157 ball types with different diameters, which were built using only brick mix (BM) soil.
158 Poisson's ratio of these clay balls should be equal since it is not a function of physical
159 characteristics of clay balls. This variation between failure polar force and square diameter
160 provides a better agreement with conditions discussed in Eq. 3. The tensile yield strength of
161 100% brick mix clay pebbles is 145kN/m^2 , according to Fig. 5. Fluctuation of points in Fig. 5

162 may be results of uncertainties associated with the PIV analysis and the controlled
163 experiment environment. Since there is a negligible diversion, this proposed method for
164 estimating the tensile yield strength of the composite clay pebbles is used in this paper.

165

166 *Effects of Burning Temperature*

167 Burning temperature of the clay pebbles is a critical factor, which maintains long-term
168 performing of water treatment process at service stage. Rajapakse et al. (2012) discussed the
169 influence of burning temperature on failure polar force of composite clay pebbles. Fig. 6
170 illustrates the tensile yield strength distribution under different burning temperatures of
171 composite clay pebbles with 50mm diameter. Previous studies (Rajapakse et al., 2012) also
172 showed that clay balls burnt at a temperature of 850 °C and above can provide sufficient
173 strength to be used as filter media. The tensile yield strength reduces by nearly 54% when
174 burning temperature increased from 800 °C to 1000 °C, while it dramatically increases by
175 approximately 287% after a 100°C burning temperature increment from 1000°C as shown in
176 Fig. 6. It is possible that cracks may have developed in clay balls due to various reasons, such
177 as excess water content. These cracks could serve as weak joints within clay balls and
178 rupture through these cracks early during testing, whereas, when balls were fired beyond
179 1000°C complete vitrification takes place increasing the tensile yield strength. The effect of
180 additional materials on tensile strength is shown in Figures 7-11. Sludge is non-plastic
181 weaker material compared to BM and RM. So adding Sludge to BM, the tensile yield
182 strength of BM-Sludge mixture can be much less than BM+RM as shown in Figure 7.
183 Tensile yield strength of BM (100%) decreases by adding RM. RM increases the elastic
184 properties of BM that could reduce the Tensile strength (Figure 8). Adding industry wastes
185 to BM or the mixture of BM-RM, the tensile yield strength decreases as it increase the voids

186 in the ball after burning at high temperature. Often, the tensile yield strengths of saturated
187 (wet) balls are slightly higher than those of dry balls. Curing the balls in water can enhance
188 the cementitious bonding between particles to increase the tensile strength of balls (Figure
189 10).

190

191 *Effects of Additional Materials*

192 Fig. 7 illustrates the influence of additional materials: red mud (RM) and sludge (S) added
193 with brick mix soil as the first step to make the composite clay pebbles in this study with
194 50mm diameter and 800⁰C burning temperature. After introducing these two additional
195 materials, the tensile yield strength of the mono-medium brick mix clay pebbles decreases
196 with portion increment of additional material as given in Fig. 7. The tensile yield strength
197 gradually reduces with red mud portion until adding 50% of red mud into the mono-medium
198 brick mix clay pebbles, where the tensile yield strength changes from 1354 kN/m² to 1086
199 kN/m² nearly by 20%. After further adding extra 25% of red mud into 50% red mud clay
200 mixture, the tensile yield strength enhance by 67% from 1086 kN/m² as shown in Fig. 7.
201 With totally replacing brick mix by red mud with same similar diameter and burning
202 temperature, the tensile yield strength of clay pebbles reduce from 1354 kN/m² to 170 kN/m²
203 by 88 percentage.

204 Impact of sludge on brick mix in clay pebble's tensile yield strength is critical
205 compared to influence of red mud, where even after adding 25% of sludge to brick mix, the
206 tensile yield strength reduces from 1354 kN/m² to 249 kN/m² by 82%, while after adding
207 50% of red mud, it reduces by 20%. Further increase of sludge percentage becomes
208 significant since the tensile yield strength reduces by 98% after adding 50% of sludge into
209 brick mix soil as shown in Fig. 7. Due to such reduction, influence of 75% and 100% sludge

210 with brick mix in the tensile yield strength is not considered in this study. Considering facts
211 as higher tensile yield strength and lower clay pebble preparation cost, soil mixture of 25% of
212 brick mix and 75% of red mud is the best material proportion for composite clay pebbles.

213

214 *Effects of Industry Wastes*

215 In second stage of the composite clay pebbles preparation, three different industry wastes: 2%
216 of shredded paper, 4% of saw dust, and 2% of sugar mulch were introduced. This new
217 material mixture modification allows enhancing the sustainability of the composite clay
218 pebbles in the water treatment process in the slow sand filters. Fig. 8 shows the impacts of
219 induced industry wastes on the tensile yield strength of the mono-medium brick mix clay
220 pebbles and the composite clay pebbles with brick mix and red mud. The tensile yield
221 strength of the mono-medium brick mix clay pebbles reduces with the industry wastes as
222 55%, 37%, and 78% for shredded paper, saw dust, and sugar mulch, respectively, as shown in
223 Fig. 8. Due to lack of the material availability of sugar mulch, only three different composite
224 clay pebbles with sugar mulch were tested in this study. Influence of rest of the industry
225 waste materials in 100% red mud on the tensile yield strength is negligible. After introducing
226 2% of shredded paper into brick mix and red mud soil mixture, the tensile yield strength of
227 these composite clay pebbles gradually decreases as in Fig. 8. The tensile yield strength of
228 clay pebbles reduce from 1354 kN/m^2 to 1124 kN/m^2 after introducing 25% of red mud into
229 100% brick mix soil, however after adding 2% of shredded paper into above two clay pebble
230 materials, the tensile yield strength of clay pebbles increase from 618 kN/m^2 to 853 kN/m^2
231 respectively. 75% of the tensile yield strength reduction surprisingly appears in clay pebbles
232 with 25% brick mix and 75% red mud through an addition of 2% of shredded paper.

233 Impact of saw dust in clay pebbles shows an opposite behavior compared to shredded
234 paper, where reduction pattern of the tensile yield strength of both composite clay pebbles
235 with brick mix and red mud soil mixture and after adding 4% of saw dust has a similar
236 behavior as illustrated in Fig. 8. After mixing 4% saw dust, the tensile yield strength
237 decreases by 37%, 34%, 8%, and 18% in composite clay pebble with 0%, 25%, 50%, and
238 75% red mud proportion, respectively. Influence of sugar mulch in the tensile yield strength
239 has totally separated performance compared to both shredded paper and saw dust, where after
240 adding 2% of sludge mulch for brick mix and red mud soil mixture, the tensile yield strength
241 regularly increases with portion of red mud in the composite clay pebbles as in Fig. 8. This
242 impact on the tensile yield strength is however insignificant compared to the influence caused
243 by shredded paper and saw dust. Concerning all these facts, best material proportion for
244 composite clay pebbles with red mud and industry wastes is 25% brick mix, 75% red mud
245 with 4% saw dust.

246 As shown in Fig. 7, sludge creates a significant impact on the tensile yield strength
247 and only three different composite clay pebbles were prepared due to such higher strength
248 reduction. To evaluate the influence of industry wastes in composite clay pebbles with
249 sludge, shredded paper, saw dust, and sugar mulch were introduced for soil mixtures and
250 evaluated the tensile yield strength of each clay pebble group as illustrated in Fig. 9. The
251 tensile yield strength of clay pebbles decreases by 44%, 26%, and 68% after adding 2% of
252 shredded paper, 4% of saw dust, and 2% of sugar mulch into the composite clay pebbles soil
253 mixture with 25% sludge and 75% brick mix. The influence of these three industry wastes in
254 50% sludge and 50% brick mix soil mixture can be negligible as given in Fig. 9.

255 Detailed analysed results of Fig. 7, Fig. 8, and Fig. 9 describe the impacts of red mud,
256 sludge, and three different industry wastes: shredded paper, saw dust, and sugar mulch on the
257 composite clay pebble with brick mix soil. Best suitable sustainable material proportion for

258 the composite clay pebbles for the preliminary water treatment in slow sand filters is 25%
259 brick mix and 75% red mud with 4% saw dust due to its higher tensile yield strength, lower
260 cost, and lower environmental pollution.

261

262 *Effects of Moisture in Composite Clay Pebbles*

263 Long-term performance of the composite clay pebbles as preliminary treatment process in
264 water treatment plants with the slow sand filters depends on performance in both construction
265 and operating stages. Strength characteristics of hand-made clay pebbles can significantly
266 affect under soaking conditions, according to past experience in Sri Lanka (Rajapakse et al.
267 2012; Rajapakse 2011). To estimate the influence of moisture on the tensile yield strength of
268 the composite clay pebbles, the tensile yield strength of clay pebbles estimated under fully
269 saturated conditions soaked for 35 days. Fig. 10 and Fig. 11 illustrate the variation of the
270 tensile yield strength of clay pebbles under fully dried and saturated conditions with red mud
271 and sludge, respectively. Impact of moisture on the tensile yield strength of the composite
272 clay pebbles with 100% red mud, 2% sugar mulch in all material proportions, 50% brick mix-
273 50% red mud with all industry wastes, 25% brick mix-75% red mud without any industry
274 waste is negligible, according to Fig. 10.

275 The tensile yield strength reduces by 6% and 11% in 100% brick mix and 4% saw
276 dust (100% brick mix) clay pebbles correspondingly under the fully saturated conditions.
277 After introducing shredded paper for 100% brick mix clay pebbles, strength however
278 enhances by 30% under fully saturated conditions compared to fully dry tensile yield strength
279 and similar behaviour shows with 25% brick mix-75% red mud with same industry waste as
280 shown in Fig. 10. As expected with moisture, the tensile yield strength of clay pebbles with
281 25% brick mix-75% red mud with 4% saw dust still reduces from 1486 kN/m² to 1299 kN/m²

282 by 13 percent. 2% of shredded paper wastes show a better performance compared to other
283 industry wastes since it can enhance the tensile yield strength characteristics of hand-made
284 clay pebbles under soaking conditions, which is more valuable in water treatment process,
285 where strength reduction is a serious problem in long-term performance. 25% brick mix-75%
286 red mud with 4% saw dust are still having 52% higher tensile yield strength than 25% brick
287 mix-75% red mud with 2% shredded paper, even after 13% strength reduction under soaking
288 conditions.

289 To evaluate the influence on moisture in the tensile yield strength degradation process
290 of clay pebbles with sludge, only 75% brick mix-25% sludge clay pebble type was examined
291 in this study since the tensile yield strength of 50% brick mix-50% sludge clay pebble, even
292 under fully dry condition is negligible as in Fig. 7. Composite clay pebbles with sludge has a
293 different behaviour compared to red mud under fully saturated conditions. After adding 2%
294 shredded paper and 4% saw dust, the tensile yield strength of saturated clay pebbles degrades
295 by 14% and 12%, respectively from its dry strength values. Under soaked conditions, the
296 strength of clay pebbles enhance by 46% and 15% with only sludge and 2% sugar mulch as
297 shown in Fig. 11.

298

299 Impacts of moisture in the tensile yield strength degradation of different composite
300 clay pebble types under soaked conditions is important to choose best material mixture for
301 water treatment plant with slow sand filters for using as preliminary filter material. After
302 analysing the tensile yield strength values of composite clay pebbles with different material
303 types and combinations under fully dry and saturated conditions from Fig. 7 to Fig. 11, 25%
304 brick mix-75% red mud with 4% saw dust is best material combination for achieving a higher
305 performance in water treatment process at both construction and operation stages.

306

307 **Conclusions**

308 Based on the analysis of calculated the tensile yield strength of composite clay balls under
309 dry and saturated condition, following conclusions are drawn:

310 • Particle image velocimetry (PIV) method is suitable to evaluate both lateral and
311 vertical strain distributions of composite clay pebbles for Poisson's ratio calculation.

312

313 • Tensile yield strength of clay pebbles reduces by 54% with burning temperature
314 increment from 800⁰C to 1000⁰C, however it reaches to its maximum as 1023.33
315 kN/m², when burning temperature is 1100⁰C due to change of material characteristics
316 by higher burning temperature. Considering the tensile yield strength, cost, and
317 environment pollution, it is recommended that 800⁰C as the best burning temperature
318 for composite clay pebbles.

319

320 • Additional of industry wastes such as red mud and sludge can significantly impact on
321 tensile yield strength of hand-made clay pebbles. There is significant the tensile yield
322 strength degradation by the addition of sludge. Composite clay balls with 25% brick
323 mix and 75% red mud proportions provide much stronger material as a filter material

324

325

326

327

328

329 **Acknowledgements**

330 This research work was carried out with the finance received from Early Career Academic
331 Recruitment and Development (ECARD) Grant from Queensland University of Technology
332 (QUT), Brisbane, Australia.

333

334 **Notation**

335 *The following symbols are used in this paper:*

336 d, D = diameter;

337 ϵ_x = lateral strain;

338 ϵ_y = vertical strain;

339 F_s = failure polar force;

340 L = patch size;

341 μ = Poisson's ratio;

342 ρ_{pixel} = precision error and

343 T_s = tensile yields strength.

344

345

346

347

348 **References**

- 349 Adrian, R. J. (1991). Particle-imaging techniques for experimental fluid mechanics. Annual
350 review of fluid mechanics, 23, 261-304, DOI: 10.1146/annurev.fl.23.010191.001401
- 351 Bandula-Heva, T., and Dhanasekar, M. (2011). Determination of stress-strain characteristics
352 of railhead steel using image analysis. World Academy of Science, Engineering and
353 Technology, 60, 1884-1888.
- 354 Hosseini, A., Mostofinejad, D., and Hajjalilue-Bonab, M. (2014). Displacement and Strain
355 Field Measurement in Steel and RC Beams Using Particle Image Velocimetry. Journal of
356 Engineering Mechanics 140, 4014086. doi:10.1061/(ASCE)EM.1943-7889.0000805
- 357 Indraratna, B., and Radampola, S. (2002). Analysis of Critical Hydraulic Gradient for Particle
358 Movement in Filtration. Journal of Geotechnical and Geoenvironmental Engineering 128,
359 347–350. doi:10.1061/(ASCE)1090-0241(2002)128:4(347)
- 360 Madabhushi, S.P.G. (2014). Centrifuge Modelling for Civil Engineers, CRC Press/Taylor &
361 Francis, Chapter 8, Centrifuge instrumentation, 111-130, ISBN 9780415668248
- 362 Pan, B., Qian, K., Xie, H., and Asundi, A. (2009). Two-dimensional digital image correlation
363 for in-plane displacement and strain measurement: a review. Measurement science and
364 technology, 20, 062001(17pp).
- 365 Rajapakse, J. (2011). Handmade clay balls and recycled crush glass as alternative media in
366 water filtration. In Kocabas, Ibrahim (Ed.) World Academy of Science, Engineering and
367 Technology. Proceedings, World Academy of Science, Engineering and Technology
368 (WASET), Phuket, Thailand, 1391-1396.

369 Rajapakse, J. and Fenner, R. (2011). "Evaluation of Alternative Media for Pebble Matrix
370 Filtration Using Clay Balls and Recycled Crushed Glass." *J. Environ. Eng.*,
371 10.1061/(ASCE)EE.1943-7870.0000350, 517-524.

372 Rajapakse, J.P., Gallage, C., Dareeju, B., Madabhushi, G., and Fenner, R. (2015). Strength
373 properties of composite clay balls containing additives from industry wastes as new filter
374 media in water treatment, *Geomechanics and Engineering*, 8(6), 859-872.

375 Rajapakse, J.P., and Ives, K.J. (1990). Prefiltration of very highly turbid waters using pebble
376 matrix filtration. *Water Environmental Journal*, 4(2),140-147.doi:10.1111/j.1747-
377 6593.1990.tb01569.x

378 Rajapakse, J. P., and Ives, K. J. (2003). "Field trials of a simple surface water treatment
379 package for rural supply (Part I)." *Environ. Eng.*, 4(1), 16–20.

380 Rajapakse, J. P., Jovanović, B., and Ljubisavljević, D. (2005). "Field trails of a simple
381 surface water treatment package for rural supply (Part II), Pebble matrix filtration field trials
382 in Serbia and Montenegro." *Environ. Eng.*, 6(3), 17–19.

383 Rajapakse, J., Madabhushi, G., Fenner, R., and Gallage, C. (2012) Properties of hand-made
384 clay balls used as a novel filter media. *Geomechanics and Engineering*, 4(4), pp. 281-294.

385 Sternberg, E. and Rosenthal, F. (1952). The elastic sphere under concentrated loads, *J. appl.*
386 *Mech.* 19 (4), 413-421.

387 Thamboo, J. A., Dhanasekar, M., and Yan, C. (2013) Effects of joint thickness, adhesion and
388 web shells to the face shell bedded concrete masonry loaded in compression. *Australian*
389 *Journal of Structural Engineering*, 14(3), 291-302.

390 Westgate, Z., and DeJong, J. (2006) Evolution of Sand-Structure Interface Response during
391 Monotonic Shear Using Particle Image Velocimetry. GeoCongress 2006: pp. 1-6. doi:
392 10.1061/(ASCE) 40803(187)277

393 White, D.J. and Take, W.A. (2002). GeoPIV: particle image velocimetry (PIV) software for
394 use in geotechnical testing (Technical Report)," Cambridge University Department of
395 Engineering.

396 White, D.J., Take,W.A., and Bolton, M.D. (2003). Soil deformation measurement using
397 particle image velocimetry (PIV) and photogrammetry, Geotechnique, 53, 619-631.

398

399

400

401

402

403

404

405

406

407

408

409

410 Table 1. Basic material properties

411

Material	d10 (mm)	d30 (mm)	d60 (mm)	Cu	Cc	PL (%)	LL (%)	size range (mm)
Brick Mix	0.075	0.200	0.600	8	0.89	16	34	-
Red mud	0.002	0.005	0.022	11	0.46	35	75	-
Sludge	0.110	0.350	1.100	10	1.01	N/A	75	-
Sugar Mulch	-	-	-	-	-	-	-	50-100
Saw dust	-	-	-	-	-	-	-	50-100

412

413

414

415

416

417

418

419

420

421

422

423 Table 2 Poisson's ratio of clay balls (Brick mix) with ball diameter

424

425

Targeted Diameter (mm)	Achieved Diameter (mm)	Failure polar force, F_s (kN)	Poisson's ratio, ν
20	28 ± 0.69	1.84 ± 0.01	0.21 ± 0.02
30	35 ± 0.46	2.41 ± 0.03	0.23 ± 0.01 ⁴²⁸
40	44 ± 0.95	3.96 ± 0.24	0.25 ± 0.01
50	54 ± 1.36	5.81 ± 0.13	0.23 ± 0.01 ⁴²⁹
60	64 ± 0.38	8.80 ± 0.09	0.22 ± 0.02 ⁴³⁰

431

432

433

434

435

436

437

438

439

440

441

442 Table 3. Poisson's ratio values of composite clay balls

Brick Mix (%)	Additional Material		Industry Waste			Poisson's ratio
	Red Mud (%)	Sludge (%)	Shredded	Saw	Sugar	
			Paper (%)	Dust (%)	Mulch (%)	
100	0	-	-	-	-	0.23
75	25	-	-	-	-	0.20
50	50	-	-	-	-	0.18
25	75	-	-	-	-	0.16
0	100	-	-	-	-	0.15
100	0	-	2	-	-	0.24
75	25	-	2	-	-	0.21
50	50	-	2	-	-	0.18
25	75	-	2	-	-	0.17
0	100	-	2	-	-	0.16
100	0	-	-	4	-	0.25
75	25	-	-	4	-	0.23
50	50	-	-	4	-	0.20
25	75	-	-	4	-	0.17
0	100	-	-	4	-	0.18
100	0	-	-	-	2	0.24
75	25	-	-	-	2	0.22
50	50	-	-	-	2	0.19
75	-	25	-	-	-	0.16
50	-	50	-	-	-	0.13
75	-	25	2	-	-	0.20
50	-	50	2	-	-	0.15
75	-	25	-	4	-	0.22
50	-	50	-	4	-	0.17
75	-	25	-	-	2	0.19
50	-	50	-	-	2	0.15

List of Figures

444

445

446 Fig. 1. Typical experimental setup for UCS and PIV experiments

447 (a) Experimental set-up

448 (b) Composite clay ball in UCS apparatus prior to loading

449 Fig. 2. Grid of patches of digital image in PIV analysis

450 Fig. 3. Vertical strain comparison between PIV and experimental methods

451 Fig. 4. Vertical strain and lateral strain distribution

452 Fig. 5. Variation of failure polar force with diameter square of clay pebbles

453 Fig. 6. Effects of burning temperature on tensile yield strength of composite clay pebbles

454 Fig. 7. Effects of additional materials on composite clay pebbles

455 Fig. 8. Effects of industry wastes with red mud

456 Fig. 9. Effects of industry wastes with sludge

457 Fig. 10. Effects of moisture on tensile yield strength degradation process with red mud

458 Fig. 11. Effects of moisture on tensile yield strength degradation process of clay ball (75%

459 Brick Mix and 25% Sludge Mix) with different industrial waste

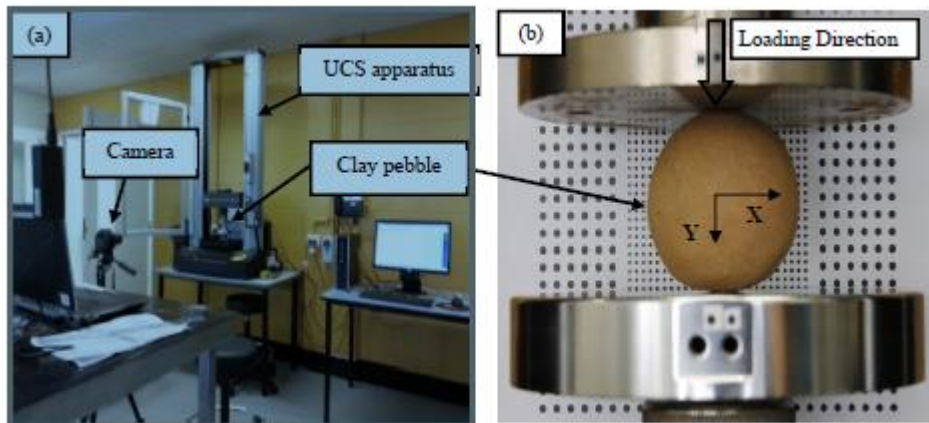
460

461

462

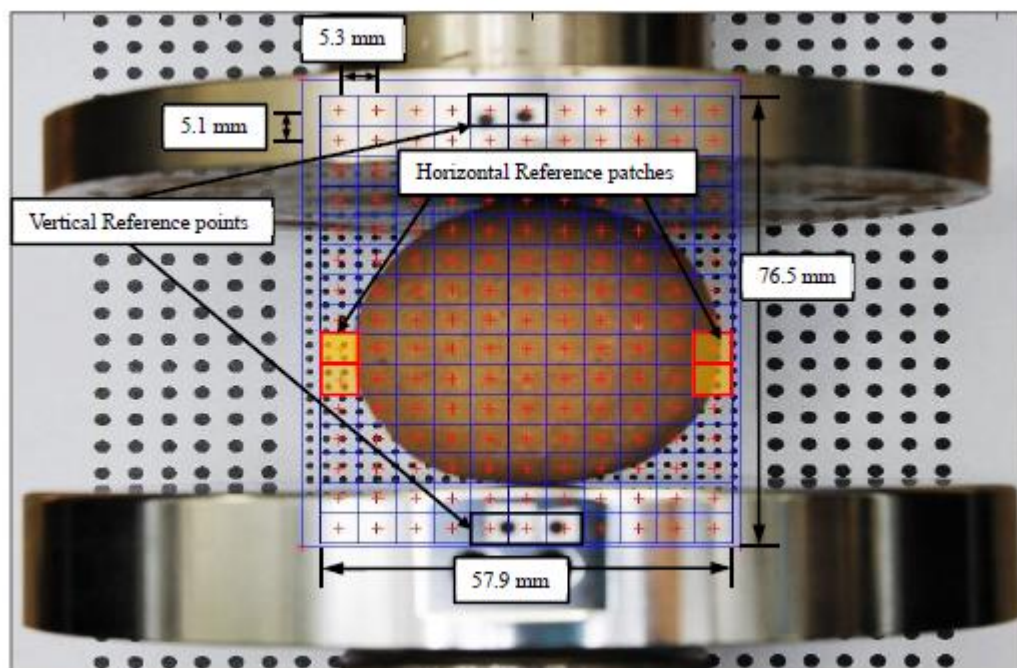
463

464 Figure 1



465

466 Figure 2



467

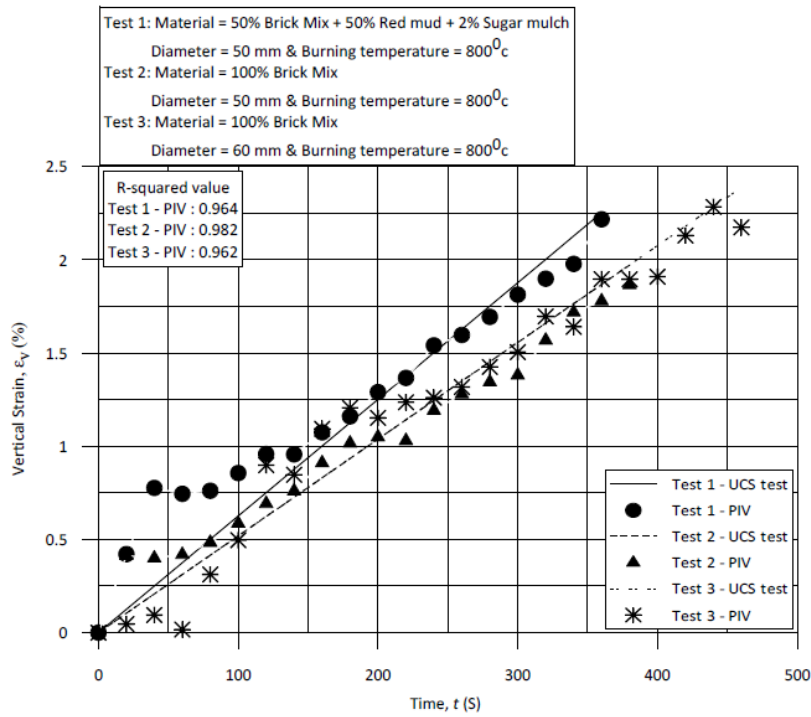
468

469

470

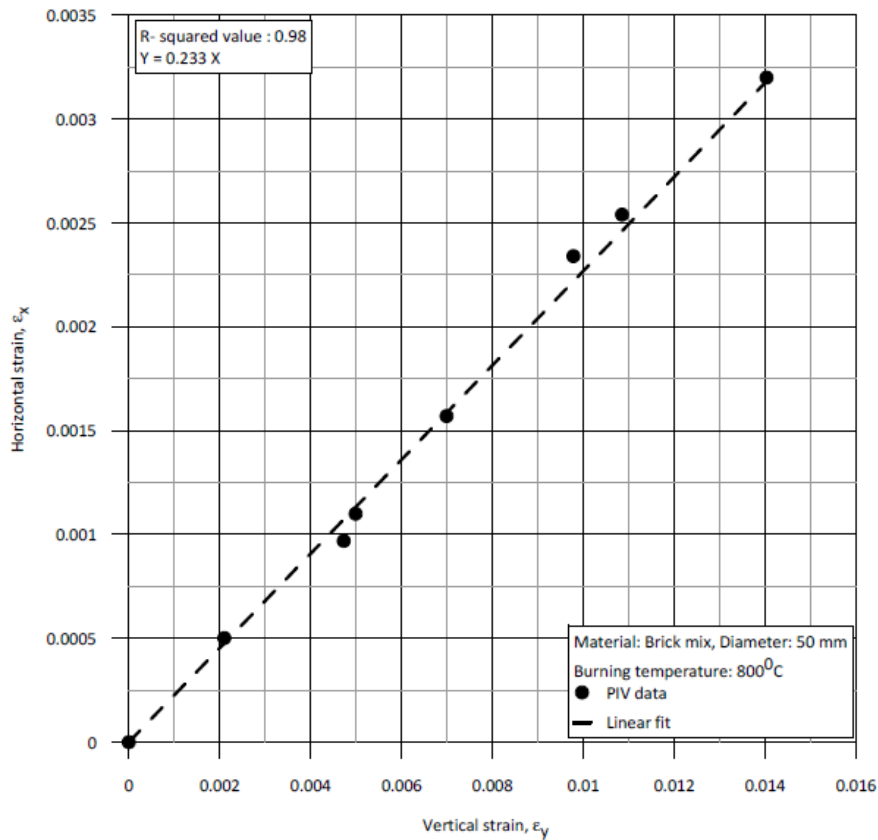
471

472 Figure 3



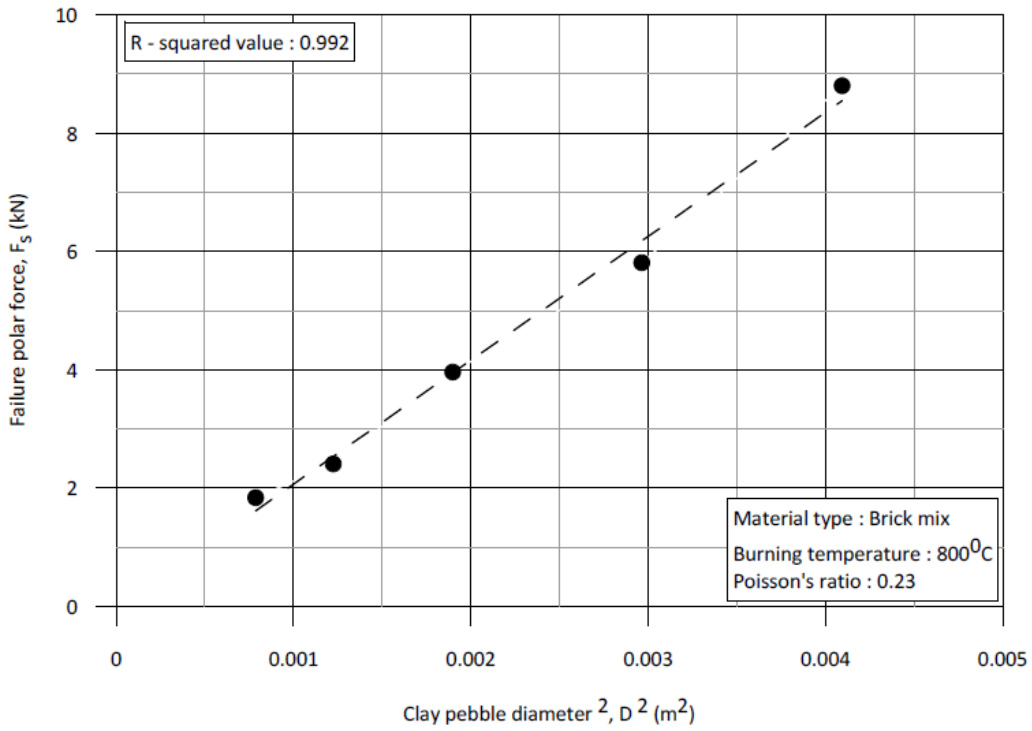
473

474 Figure 4



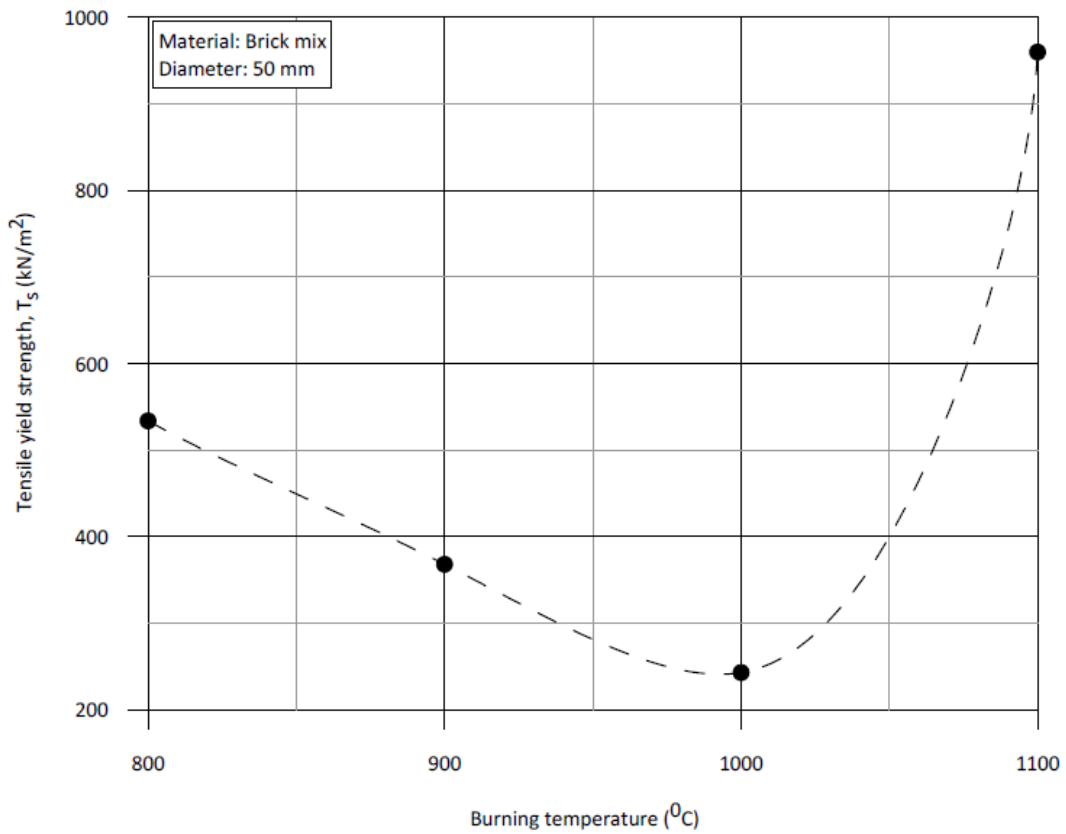
475

476 Figure 5



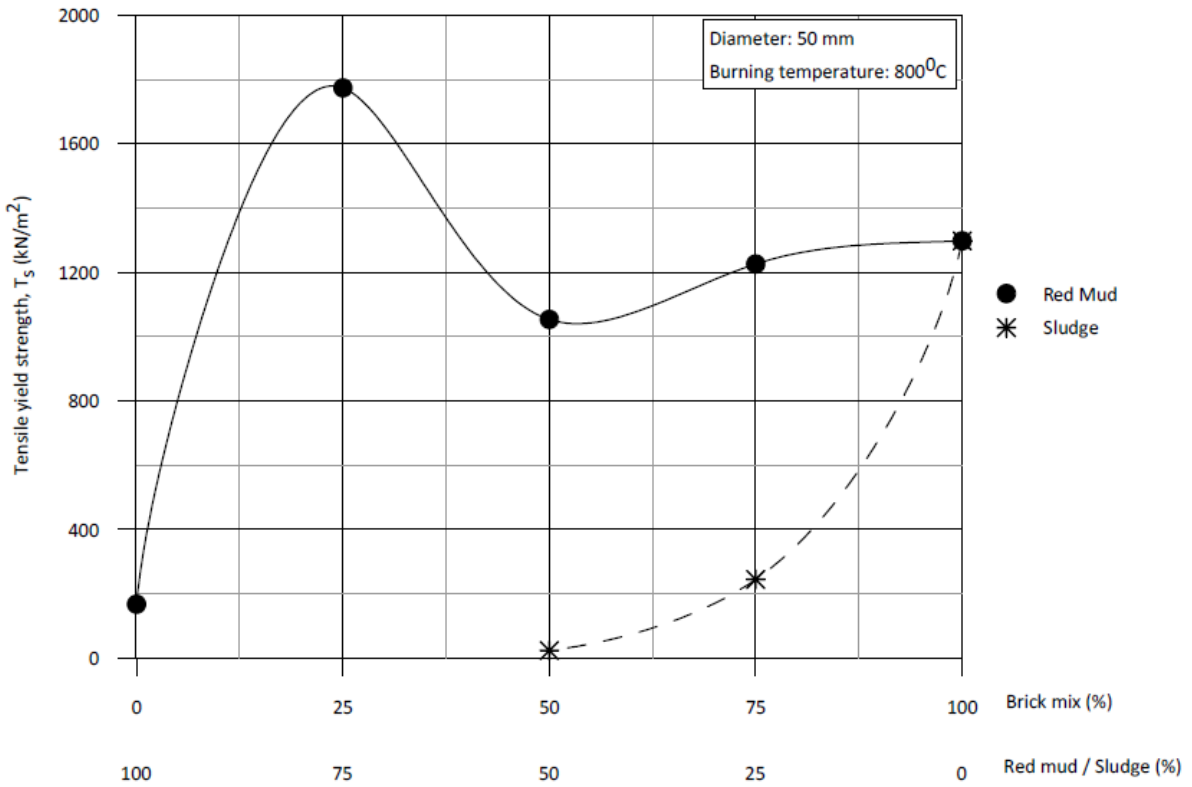
477

478 Figure 6



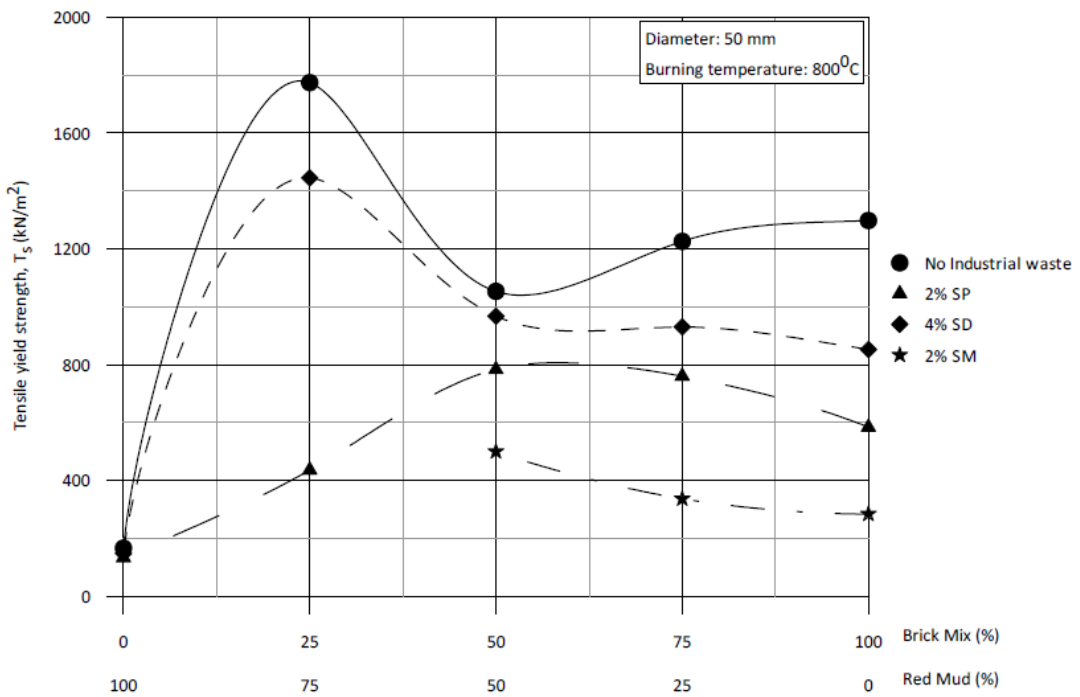
479

480 Figure 7



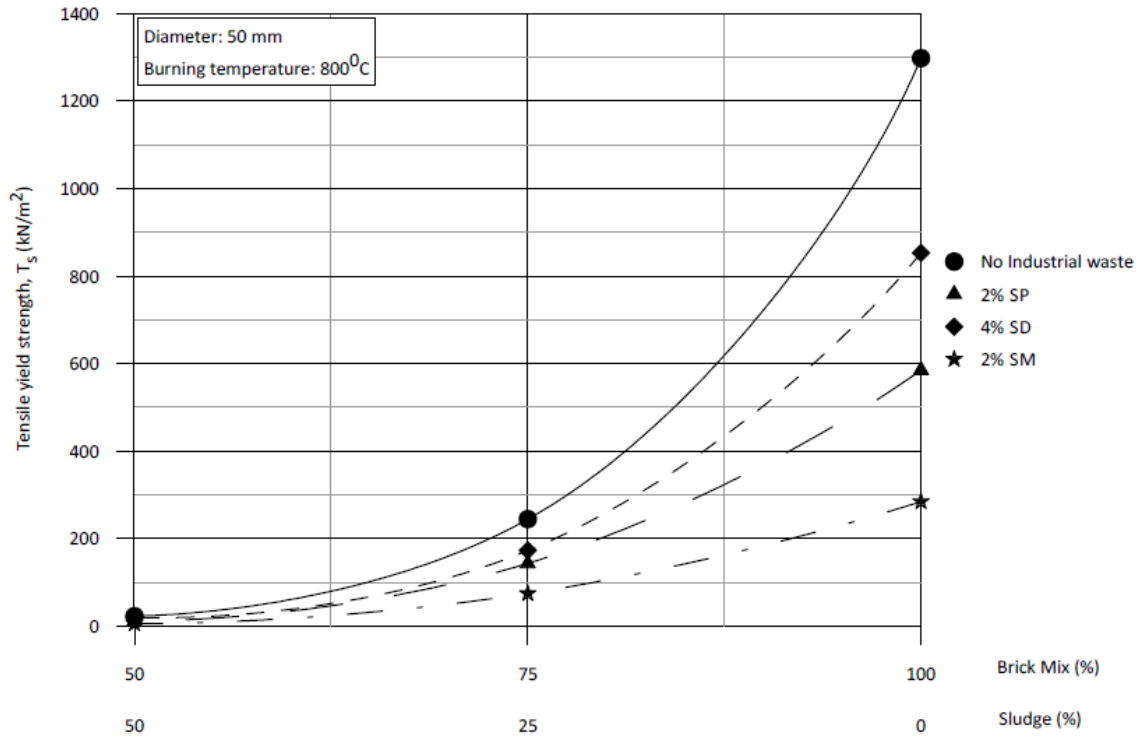
481

482 Figure 8



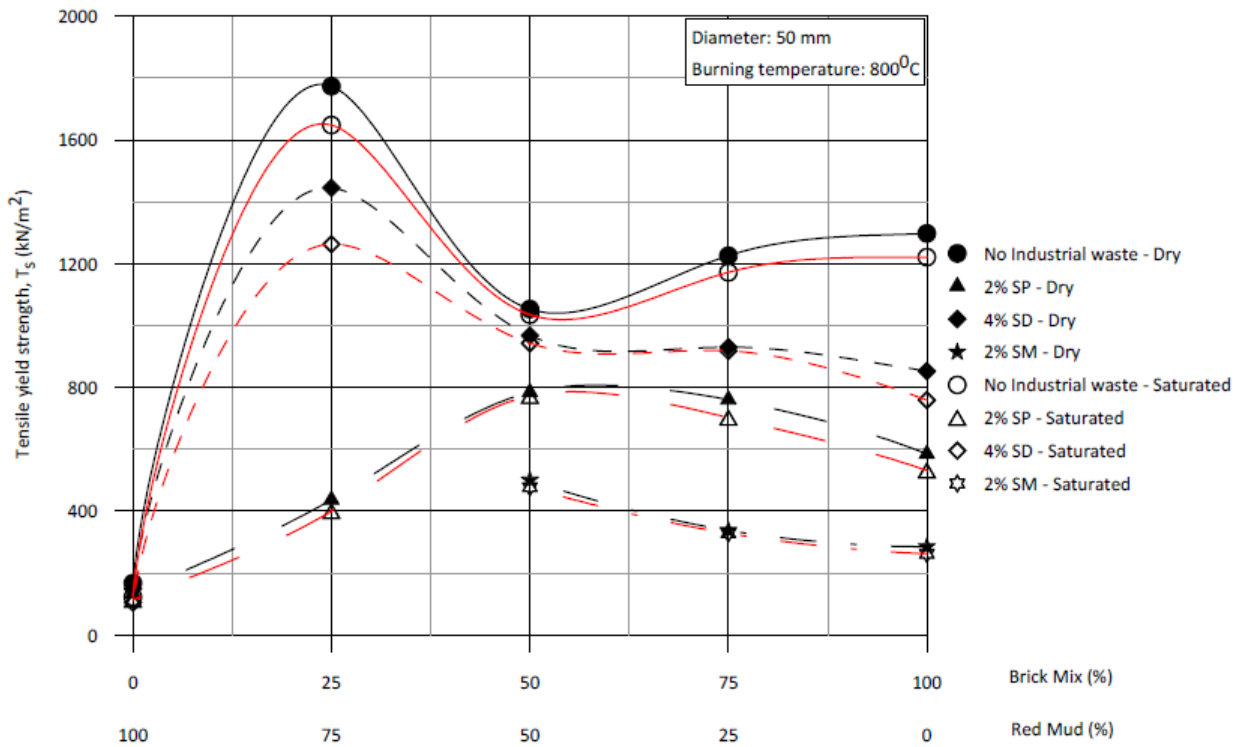
483

484 Figure 9



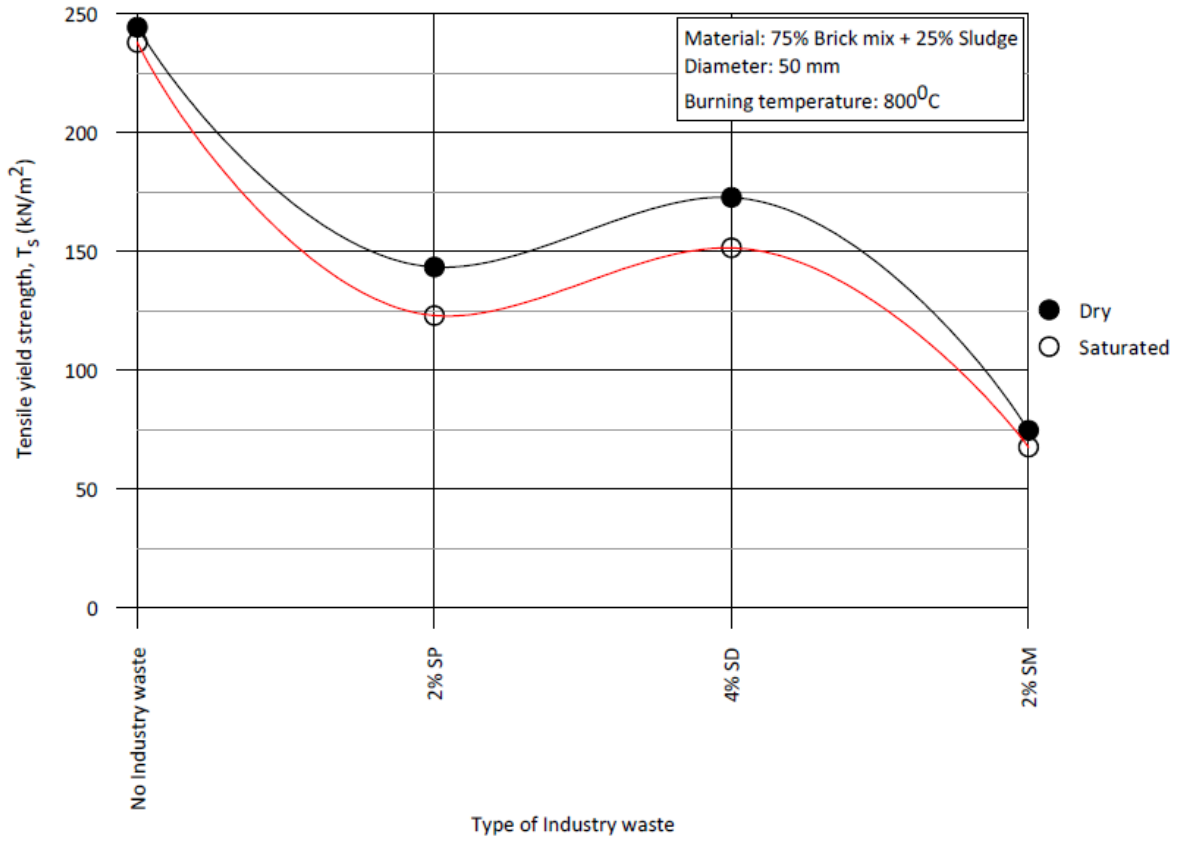
485

486 Figure 10



487

488 Figure 11



489